World Academy of Science, Engineering and Technology
International Journal of Mechanical and Mechatronics Engineering
Vol:8, No:5, 2014

Numerical Investigation of Poling Vector Angle on Adaptive Sandwich Plate Deflection

Alireza Pouladkhan, Mohammad Yavari Foroushani, Ali Mortazavi

International Science Index, Mechanical and Mechatronics Engineering Vol:8, No:5, 2014 waset.org/Publication/9998135

***Abstract*—**This paper presents a finite element model for a Sandwich Plate containing a piezoelectric core. A sandwich plate with a piezoelectric core is constructed using the shear mode of piezoelectric materials. The orientation of poling vector has a significant effect on deflection and stress induced in the piezo-actuated adaptive sandwich plate. In the present study, the influence of this factor for a clamped-clamped-free-free and simple-simple-free-free square sandwich plate is investigated using Finite Element Method. The study uses *ABAQUS* (*v.6.7*) software to derive the finite element model of the sandwich plate. By using this model, the study gives the influences of the poling vector angle on the response of the smart structure and determines the maximum transverse displacement and maximum stress induced.

***Keywords*—**Finite element method, Sandwich plate, Poling vector, Piezoelectric materials, Smart structure, Electric enthalpy.

I. Introduction

SHEAR piezoelectric actuators have been used to generate deflection in aerospace structures. Among the items under development are variable shape inlets and control surfaces, full-span, chord-wise, span-wise contouring trailing control surfaces, buffet load alleviation, flutter suppression and flow control that use piezoelectric materials and other strain-based actuators for actuation.

In 1995, Mitchell and Reddy [1] developed a retained hybrid theory of laminated plates with piezoelectric lamina using energy principle and third-order shear deformation theory as a basic theory for shear-actuated laminated structures.

The idea of exploiting the shear mode to create transverse deflection in sandwich beams was first suggested by Sun and Zhang [2] in 1995. A commercial finite element package was used to model numerically a cantilever beam with shear piezoelectric actuator. It was shown that embedded shear actuators offer many advantages over surface mounted extension actuators. In later work, Zhang and Sun [3] in 1996 formulated an analytical model of a sandwich beam with shear piezoelectric actuator that occupies the entire core. The model derivation was simplified by assuming that the face layers follow Euler-Bernoulli beam, whereas the core layer obeys Timoshenko beam. Furthermore, a closed form solution of the static deflection was presented for a cantilever beam. A finite element approach was used by Benjeddou et al. [4] in 1997 to model a sandwich beam with shear and extension piezoelectric elements. The finite element model employed the displacement field of Zhang and Sun [3]. It was shown that the FE results supported the analytical results.

In 1999, Reddy [5] presented theoretical formulations, the Navier solutions and FE models based on the classical and shear deformation plate theories for the analysis of laminated plates with integrated sensors and actuators and subjected to both mechanical and electrical loadings. At the same year, Zhang and Sun [6] according to their two previous works, constructed a sandwich plate with a piezoelectric core using the shear mode of piezoceramic PZT4. The Rayleigh-Ritz formulation for the proposed plate was developed based on the principle of stationary potential energy for a clamped-clamped-free-free square sandwich plate. They also modeled a clamped-clamped-free-free and a cantilever sandwich plate in ABAQUS and compare the tip deflection of the proposed sandwich plate obtained from two methods.

In 2000, Benjeddou [7] published the first survey and discussed the advances and trends in the formulations and applications of the FE modeling of adaptive structural elements. He stated the specific assumptions, in particular those of electrical type and the characteristics of the elements, for most contributions and illustrated the information for helpful use by the researchers as well as the designers interested in this growing field of smart materials and structures. However, the focus was put on the development of adaptive piezoelectric finite elements only and the other methods are excluded. FE modeling of smart structures continued and developed in later years. At the same year, Chee et al. [8] developed a theoretical formulation for modeling composite smart structures, in which the piezoelectric actuators and sensors were treated as constituent parts of the entire structural system based on a high order displacement field coupled with a layer-wise linear electric potential. The model was developed for a laminated plate structure using Hamilton's variational principle with the FE formulation. They concluded that the performance of the 8 node element was found to be superior to the four node element for very thin structures.

Zhou et al. [9] used a two-way piezo-mechanical coupled theory to investigate the multiple field interactions of composite laminates with surface-bonded piezoelectric actuators and sensors. They used laminate theory accurately model transverse shear deformation which was significant in

Alireza Pouladkhan is with the Young Researchers and Elite Club, Najafabad Branch, Islamic Azad University, Najafabad, Esfahan, Iran (phone: +98-913-304-9487; e-mail: a_pouladkhan@yahoo.com).

Mohammad Yavari Foroushani is with the Young Researchers and Elite Club, Khomeinishahr Branch, Islamic Azad University, Khomeinishahr, Esfahan, Iran (e-mail: mohammad.yavari@iaukhsh.ac.ir).

Ali Mortazavi is with the Department of Civil Engineering, Power and Water University of Technology (PWUT), Tehran, Iran (e-mail: mortazavi@pwut.ac.ir).

International Science Index, Mechanical and Mechatronics Engineering Vol:8, No:5, 2014 waset.org/Publication/9998135

moderately thick constructions. They developed an FE laminate model with surface bonded/embedded piezoelectric actuators or sensors to implement the theory. Induced deformation, charge and current were investigated to evaluate actuation and sensing effects of piezoelectric materials. Numerical results indicate that two-way coupling effects affect the prediction of structural deflection, stress distribution and electrical signal significantly compared with uncoupled theory. They stated the thickness ratio of piezoelectric layer to plate structure is a critical parameter that governs the significance of coupling effects. The coupled piezo-mechanical theory is capable of accurately modeling the characteristics of thick piezoelectric layers.

Bisegna and Caruso [10] developed FE formulations for a plate having thin piezoelectric actuators bonded on its upper and/or lower surfaces.

In 2001, Huang and Sun [11] developed a refined theory and approximate analytical solutions of laminated composite structures with piezoelectric laminae using energy principle.

Kapuria [12] developed an efficient coupled electromechanical model for multilayered composite structures with embedded or surface bonded piezoelectric laminae subjected to static electromechanical excitation. The results showed significant improvement over the first order solution and compare very well with the exact solution for both thin and thick piezoelectric laminated structures. He illustrated the feasibility of controlling deflection by applying appropriate actuation potential.

Vel and Batra [13] obtained an exact solution for the three-dimensional deformations of simply supported laminated rectangular thick plates with embedded shear mode piezoelectric actuators, subjected to mechanical and electrical loading on the upper and lower surfaces. They showed exact displacements and stresses for a homogeneous piezoelectric plate for various length-to-thickness ratios were agree with those obtained by the first-order shear deformation theory. A comparison of the stresses with those in the corresponding surface-mounted extension actuation configuration illustrated that for the same transverse deflection of the plate centroid, the maximum longitudinal stress within the actuator is significantly smaller for the shear actuation mechanism.

In 2002, Wang and Quek [14] developed a mechanical based model for the flexural analysis of structures with embedded piezoelectric layers. They considered closed and open circuits to connect the electrodes on the surfaces of the piezoelectric layers. For the closed circuit case, the potential shape function was related to the transverse displacement, or more accurately the curvature of the beam. For the open circuit case, the potentials at the boundaries in the longitudinal direction were directly related to the slope of the deflection of the beam.

In 2003, Aldraihem and Khdeir [15] developed exact deflection models of beams with shear piezo-actuators with the aid of the state-space approach and Jordan canonical form. They used the first-order and higher-order beam theories to formulate the models. They showed that the first-order beam cannot predict the beam behavior when compared with the results of the higher-order beam.

In 2004, Lesieutre et al. [16] invented a nonlinear motion transmission mechanism for improving the mechanical work output of an active material drive element. The motion transmission mechanism consists of a simple linkage that couples the active material to the load. As the active material does work on the load, the linkage changes the mechanical advantage or leverage of the active material with respect to the load, thereby tailoring the load to best exploit the active material's force-displacement behavior. A kinematic model was used to predict the maximum quasi-static mechanical work output that can be obtained. Optimization of the model geometry results in a transmission with a theoretical work enhancement of 37% for a constant load, and a theoretical work enhancement that approaches 100% for a spring load.

Garcia Lage et al. [17] developed a layer-wise FE model for piezolaminated plate structures. A Reissner mixed variational principle was used to formulate the FE model. The model in contrast with the standard layer-wise displacement based FE model, fulfilled the continuity of all primary variables across the interface between adjacent layers. But they evaluated only the in-plane stress components and electric displacements in the post-computation through the piezolaminate constitutive equations.

In 2005, Kapuria and Achary [18] presented a coupled consistent third-order theory for static thermoelectromechanical response of hybrid piezoelectric laminated plates, which unlike the existing third-order theory, satisfies exactly the shear traction-free conditions at top and bottom of the hybrid plates for any electrical boundary conditions. The transverse as well as in-plane electric fields were considered in their theory. They obtained Navier-type solutions for simply-supported plates.

Azulay and Abramovich [19] investigated the behavior of a laminated composite plate with embedded or bonded piezoelectric materials. They developed an exact mathematical model based on Reissner-Mindlin theory (FSDT) for piezo-laminated composite plates. They also solved flexural behavior based on Levy method approach for plates. Therefore, the study was limited to exact solutions only for the cases of plates with at least two opposite simply-supported edges, and only continuous piezoelectric layers. They performed a comprehensive parametric investigation to study the behavior of extension or shear piezo-actuated plates with various boundary conditions using Ritz method.

In 2006, Polit and Bruant [20] invented piezoelectric extension of the FSDT eight node plate finite element. An evaluation was proposed in order to assess the best compromise between minimum number of degrees of freedom and maximum efficiency. Furthermore, at the post-processing level, the transverse shear stresses were deduced using the equilibrium equations. Finally, an adaptive composite plate was evaluated using the best compromise finite element.

Robaldo et al. [21] developed some finite elements for the analysis of laminated plates embedding piezoelectric layers based on the principle of virtual displacements (PVD) and a unified formulation.

International Science Index, Mechanical and Mechatronics Engineering Vol:8, No:5, 2014 waset.org/Publication/9998135

In 2007, Balamurugan and Narayanan [22] innovated a higher-order shear-flexible piezolaminated C1QUAD-8 multi-layer smart composite plate finite element with 48 elastic degrees of freedom and 9 electric degrees of freedom per piezoelectric layer in the element. The element was developed to include stiffness and the electromechanical coupling of the piezoelectric sensor/actuator layers.

Sheng et al. [23] established the state equation for laminated piezoelectric plate based on the theories of 3D piezoelectro-elasticity by assuming appropriate boundary functions.

Ren [24] investigated the application of a piezoelectric actuator to control deformation of thin unsymmetric cross-ply composite laminates. He or She developed theoretical model based on Rayleigh-Ritz principle to predict laminate deformation and the effect of the piezoelectric actuator layer. The bifurcation dimension increased when the thickness of piezoelectric layer increases. Laminate curvatures were in a perfectly linear relationship with an electric field applied to the piezoelectric actuator layer. Snap-through from one stable shape to the other could occur by applying an electric field.

In present study, the model made by Zhang and Sun has been simulated in *ABAQUS* (*v.6.7*) [25] software to derive the finite element model of the sandwich plate. Finally, the effect of poling vector angle on sandwich plate's deflection was investigated and proved that when plate is completely symmetric with respect to $y = x$ axis free tip deflection is increased and maximum Von-Mises stress is decreased.

II. Description of a Piezoelectric Sandwich Plate

The underlying principle of sandwich construction can be illustrated as follows. In a sandwich construction (see Fig. 1), the top and bottom layers are stiff facing sheets, and the central layer is a piezoelectric core in which the poling direction of the piezoelectric material is arranged along the x direction.

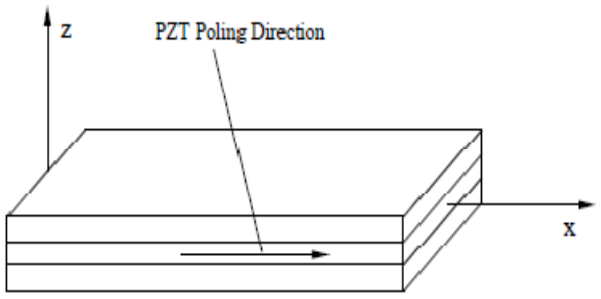

Fig. 1 Schematic diagram of the sandwich plate

When an electric field is applied along the z direction, the piezoelectric core will produce a pure shear deformation which is the driving force for the transverse deflection of the sandwich construction. The shear deformation of the core is depicted in Fig. 2.

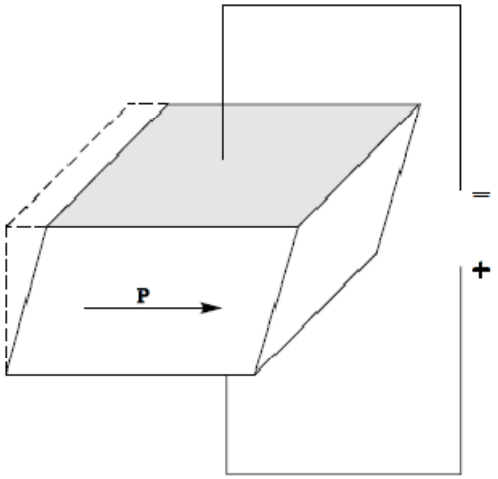

Fig. 2 Shear mode of the piezoelectric core

III. Basic Assumptions

In order to simplify the formulation procedure, the following assumptions are introduced by Zhang and Sun [6]:

(1) In each layer, the normal stress, σ_z, is assumed to vanish.
(2) The interfaces between adjacent layers are perfectly bonded.
(3) The transverse displacements (i.e. the displacement along the z direction) in the layers are equal.
(4) The top and bottom layers are assumed to be classical plates; namely, the transverse shear strains in the layers will be neglected. The central core is assumed to be a first-order shear plate, which allows the transverse shear deformation.
(5) Rotatory inertia terms are negligible.
(6) The piezoelectric material for this application is assumed to be transversely isotropic. The piezoelectric constants are e_{31} , e_{33} and e_{15}.
(7) The two surfaces of the piezoelectric layer are entirely covered with electrodes. Therefore, the electric potential will be independent of x and y locations.

IV. Piezoelectric Material Constitutive Equations and Electric Enthalpy

For piezoelectric ceramics (with $6mm$ symmetry), the materials are transversely isotropic. The constitutive relation can be represented in terms of the reduced tensor notation with respect to 1-2-3 axes of piezoelectric material:

$$T_p = c_{pq}^E S_q - e_{kp} E_k$$
$$D_i = e_{iq} S_q + \varepsilon_{ik}^S E_k \quad (1)$$

where T_p , S_q , D_i and E_k are the components of the reduced stress tensor, reduced strain tensor, electric flux density vector, and the electric field vector, respectively [26].

$$c_{ij}^{E}=\begin{bmatrix} c_{33}^{E} & c_{13}^{E} & c_{13}^{E} & 0 & 0 & 0 \\ c_{13}^{E} & c_{11}^{E} & c_{12}^{E} & 0 & 0 & 0 \\ c_{13}^{E} & c_{12}^{E} & c_{11}^{E} & 0 & 0 & 0 \\ 0 & 0 & 0 & c_{66}^{E} & 0 & 0 \\ 0 & 0 & 0 & 0 & c_{44}^{E} & 0 \\ 0 & 0 & 0 & 0 & 0 & c_{44}^{E} \end{bmatrix} \quad (2)$$

The coefficients c_{pq}^{E} are the elastic constants measured at constant electric field.

$$e_{ij}=\begin{bmatrix} e_{33} & e_{31} & e_{31} & 0 & 0 & 0 \\ 0 & 0 & 0 & 0 & 0 & e_{15} \\ 0 & 0 & 0 & 0 & e_{15} & 0 \end{bmatrix} \quad (3)$$

The components e_{iq} denote piezoelectric constants.

$$\varepsilon_{ij}^{S}=\begin{bmatrix} \varepsilon_{33}^{S} & 0 & 0 \\ 0 & \varepsilon_{11}^{S} & 0 \\ 0 & 0 & \varepsilon_{11}^{S} \end{bmatrix} \quad (4)$$

The coefficients ε_{ik}^{S} represent the components of the dielectric permittivity tensor measured at constant strain. In (2) to (4), the 1 direction is always the poling direction, and the 2-3 plane is an isotropic plane. For simplicity in notation, the superscripts in the above equation will henceforth be omitted. The electric field-electric potential relations are given by:

$$E_k=-\phi_{,k} \quad (5)$$

where ϕ is the electric potential function.

The electrical enthalpy in a piezoelectric body is an energy quantity similar to strain energy in an elastic structure. From the thermodynamic argument, it is shown that electrical enthalpy is a function of only the infinitesimal strain-tensor components S_{kl} and the electrical field intensity E_k. The simplest form of electrical enthalpy which is compatible with thermodynamics can be constructed for linear theory as [27]:

$$H=\frac{1}{2}c_{ijkl}S_{ij}S_{kl}-e_{ijk}E_iS_{jk}-\frac{1}{2}\varepsilon_{ij}E_iE_j \quad (6)$$

V. Transformed Constitutive Equations

In order to study the effect of polling vector orientation on the plate deflection, we should transform the constitutive equations and calculate the electric enthalpy and potential energy as a function of φ (see Fig. 3). The transformation matrix for rotation in 1-2 plane and unchanged axis 3 is as follows:

$$Q_{ij}=\begin{bmatrix} \cos\theta & \sin\theta & 0 \\ -\sin\theta & \cos\theta & 0 \\ 0 & 0 & 1 \end{bmatrix} \quad (7)$$

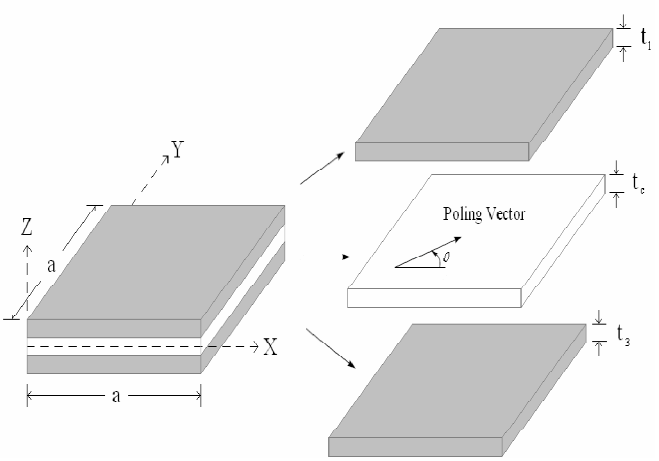

Fig. 3 Sandwich plate construction and poling vector orientation in horizontal direction

VI. Rotation of Elasticity Tensor

To use elasticity tensor transformation relations [28], we should consider the general anisotropic elasticity:

$$C_{ij}=\begin{bmatrix} C_{1111} & C_{1122} & C_{1133} & C_{1123} & C_{1131} & C_{1112} \\ & C_{2222} & C_{2233} & C_{2223} & C_{2231} & C_{2212} \\ & & C_{3333} & C_{3323} & C_{3331} & C_{3312} \\ & & & C_{2323} & C_{2331} & C_{2312} \\ & Sym. & & & C_{3131} & C_{3112} \\ & & & & & C_{1212} \end{bmatrix} \quad (8)$$

and the transformed tensor will be in the following form :

$$c'_{ij}(\theta)=\begin{bmatrix} c'_{11}(\theta) & c'_{12}(\theta) & c'_{13}(\theta) & 0 & 0 & c'_{16}(\theta) \\ & c'_{22}(\theta) & c'_{23}(\theta) & 0 & 0 & c'_{26}(\theta) \\ & & c_{11}^{E} & 0 & 0 & c'_{36}(\theta) \\ & & & c'_{44}(\theta) & c'_{45}(\theta) & 0 \\ & Sym. & & & c'_{55}(\theta) & 0 \\ & & & & & c'_{66}(\theta) \end{bmatrix} \quad (9)$$

which the transformed tensor components are :

$$c'_{11}(\theta)=c_{33}^{E}\cos^4\theta+c_{11}^{E}\sin^4\theta+(2c_{13}^{E}+4c_{44}^{E})\cos^2\theta\sin^2\theta \quad (10)$$

$$c'_{12}(\theta)=(c_{33}^{E}-4c_{44}^{E}+c_{11}^{E})\cos^2\theta\sin^2\theta+2c_{13}^{E}\sin^4\theta \quad (11)$$

$$c'_{13}(\theta)=c_{13}^{E}\cos^2\theta+c_{12}^{E}\sin^2\theta \quad (12)$$

$$c'_{14}(\theta)=c'_{15}(\theta)=0 \quad (13)$$

$$c'_{16}(\theta)=(c_{13}^{E}-c_{33}^{E}+2c_{44}^{E})\cos^3\theta\sin\theta+(c_{11}^{E}-c_{13}^{E}-2c_{44}^{E})\cos\theta\sin^3\theta \quad (14)$$

$$c'_{22}(\theta)=c_{33}^{E}\sin^4\theta+c_{11}^{E}\cos^4\theta+(2c_{13}^{E}+4c_{44}^{E})\cos^2\theta\sin^2\theta \quad (15)$$

$$c'_{23}(\theta)=c_{13}^{E}\sin^2\theta+c_{12}^{E}\cos^2\theta \quad (16)$$

$$c'_{24}(\theta)=c'_{25}(\theta)=0 \quad (17)$$

$$c'_{26}(\theta)=(c_{13}^{E}-c_{33}^{E}+2c_{44}^{E})\cos\theta\sin^3\theta+(c_{11}^{E}-c_{13}^{E}-2c_{44}^{E})\cos^3\theta\sin\theta \quad (18)$$

$$c'_{33}(\theta)=c_{11}^{E} \quad (19)$$

International Science Index, Mechanical and Mechatronics Engineering Vol:8, No:5, 2014 waset.org/Publication/9998135

$$c'_{34}(\theta) = c'_{35}(\theta) = 0 \quad (20)$$

$$c'_{36}(\theta) = (c^E_{12} - c^E_{13})cos\theta sin\theta \quad (21)$$

$$c'_{44}(\theta) = c^E_{44}sin^2\theta + c^E_{66}cos^2\theta \quad (22)$$

$$c'_{45}(\theta) = (c^E_{66} - c^E_{44})cos\theta sin\theta \quad (23)$$

$$c'_{46}(\theta) = 0 \quad (24)$$

$$c'_{55}(\theta) = c^E_{44}cos^2\theta + c^E_{66}sin^2\theta \quad (25)$$

$$c'_{56}(\theta) = 0 \quad (26)$$

$$c'_{66}(\theta) = (c^E_{33} - 2c^E_{13} - 2c^E_{44} + c^E_{11})cos^2\theta sin^2\theta + c^E_{44}(cos^4\theta + sin^4\theta) \quad (27)$$

VII. Rotation of Piezoelectricity Tensor

According the second equation (1) in absence of electric field, the third order piezoelectricity tensor relates electric flux density vector and strain tensor.

$$D_i = e_{ikl}S_{kl} \quad (28)$$

If we transform the strain tensor [29]:

$$S'_{ij} = Q_{ik}Q_{jl}S_{kl} \ , \qquad S_{ij} = Q_{ki}Q_{lj}S'_{kl} \quad (29)$$

and the flux density vector :

$$D'_i = Q_{ij}D_j \ , \qquad D_i = Q_{ji}D'_j \quad (30)$$

then put them in (28) we have :

$$Q_{ji}D'_j = e_{ikl}Q_{mk}Q_{nl}S'_{mn} \quad (31)$$

Multiply with Q_{ri} and use the orthogonality of transformation matrix yield:

$$D'_i = Q_{ir}Q_{km}Q_{ln}e_{rmn}S'_{kl} \quad (32)$$

If we compare (32) with (28) will found:

$$e'_{ikl} = Q_{ir}Q_{km}Q_{ln}e_{rmn} \quad (33)$$

which is the transformation relation of piezoelectricity tensor. The transformed tensor of (3) in the reduced matrix form will be:

$$e'_{ij}(\theta) = \begin{bmatrix} e'_{11}(\theta) & e'_{12}(\theta) & e'_{13}(\theta) & 0 & 0 & e'_{16}(\theta) \\ e'_{21}(\theta) & e'_{22}(\theta) & e'_{23}(\theta) & 0 & 0 & e'_{26}(\theta) \\ 0 & 0 & 0 & e'_{34}(\theta) & e'_{35}(\theta) & 0 \end{bmatrix} \quad (34)$$

As the transformed matrix is a combination piezoelectricity matrices for materials poled in 1 and 2 directions, places for both cases filled simultaneously. The transformed tensor components are written below:

$$e'_{11}(\theta) = e_{33}cos^3\theta + (e_{31} + 2e_{15})cos\theta sin^2\theta \quad (35)$$

$$e'_{12}(\theta) = (e_{33} - 2e_{15})cos\theta sin^2\theta + e_{31}cos^3\theta \quad (36)$$

$$e'_{13}(\theta) = e_{31}cos\theta \quad (37)$$

$$e'_{14}(\theta) = e'_{15}(\theta) = 0 \quad (38)$$

$$e'_{16}(\theta) = (e_{31} - e_{33} + e_{15})cos^2\theta sin\theta - e_{15}sin^3\theta \quad (39)$$

$$e'_{21}(\theta) = (2e_{15} - e_{33})cos^2\theta sin\theta - e_{31}sin^3\theta \quad (40)$$

$$e'_{22}(\theta) = -e_{33}sin^3\theta - (e_{31} + 2e_{15})cos^2\theta sin\theta \quad (41)$$

$$e'_{23}(\theta) = -e_{31}sin\theta \quad (42)$$

$$e'_{24}(\theta) = e'_{25}(\theta) = 0 \quad (43)$$

$$e'_{26}(\theta) = (e_{33} - e_{31} - e_{15})cos\theta sin^2\theta + e_{15}cos^3\theta \quad (44)$$

$$e'_{31}(\theta) = e'_{32}(\theta) = e'_{33}(\theta) = 0 \quad (45)$$

$$e'_{34}(\theta) = -e_{15}sin\theta \quad (46)$$

$$e'_{35}(\theta) = e_{15}cos\theta \quad (47)$$

$$e'_{36}(\theta) = 0 \quad (48)$$

VIII. Rotation of Dielectric Tensor

Dielectric is a second order tensor and would be transformed as follows:

$$\varepsilon'_{ml} = Q_{mi}Q_{lk}\varepsilon_{ik} \quad (49)$$

So, the transformed tensor of (4) will be:

$$\varepsilon'_{ij}(\theta) = \begin{bmatrix} \varepsilon'_{11}(\theta) & \varepsilon'_{12}(\theta) & 0 \\ & \varepsilon'_{22}(\theta) & 0 \\ Sym. & & \varepsilon^S_{11} \end{bmatrix} \quad (50)$$

which the transformed tensor components are:

$$\varepsilon'_{11}(\theta) = \varepsilon_{33}cos^2\theta + \varepsilon_{11}sin^2\theta \quad (51)$$

$$\varepsilon'_{12}(\theta) = (\varepsilon_{11} - \varepsilon_{33})cos\theta sin\theta \quad (52)$$

$$\varepsilon'_{13}(\theta) = 0 \quad (53)$$

$$\varepsilon'_{22}(\theta) = \varepsilon_{11}cos^2\theta + \varepsilon_{33}sin^2\theta \quad (54)$$

$$\varepsilon'_{23}(\theta) = 0 \quad (55)$$

$$\varepsilon'_{33}(\theta) = \varepsilon^S_{11} \quad (56)$$

IX. Geometry and Problem Description

In this section, a special clamped-clamped-free-free square sandwich plate will be studied. The geometrical configuration of the sandwich plate is shown in Fig. 3. The boundary configuration of the sandwich plate is shown in Fig. 4.

International Science Index, Mechanical and Mechatronics Engineering Vol:8, No:5, 2014 waset.org/Publication/9998135

International Science Index, Mechanical and Mechatronics Engineering Vol:8, No:5, 2014 waset.org/Publication/9998135

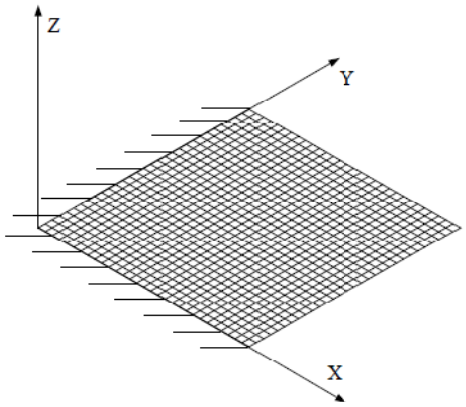

Fig. 4 Boundary configuration of the fixed-fixed-free-free sandwich plate

The length of the square sandwich plate is assumed to be 3.0cm. The total thickness of the sandwich plate is 0.3cm, with each of the cover sheets and the core being 0.1cm. The skew angle of the poling direction of the piezoelectric layer with respect to the x direction, φ, is $0-90^{\circ}$. The cover sheets of the sandwich plate are assumed to be aluminum with a Young's modulus of 70.3 GPa and a Poisson's ratio of 0.345. The piezoelectric layer is PZT4 piezoceramic. The mechanical properties of the PZT4 material are listed in Table I [30].

TABLE I
MECHANICAL PROPERTIES OF PIEZOCERAMIC PZT-4

c_{11}	c_{12}	c_{13}	c_{33}	c_{44}
13.9	7.78	7.40	11.5	2.56
		$\times 10^{10}\ N/m^2$		
e_{31}	e_{33}	e_{15}	ε_{11}	ε_{33}
−5.2	15.1	12.7	0.646	0.562
	C/m^2		$\times 10^{-8}\ C/Vm$	

There is a voltage of 10000 volts applied between the top and bottom surfaces of the central piezoelectric layer.

At first, we want to investigate the effect of poling vector direction on deflection and stress induced in the piezo-actuated adaptive sandwich plate for a Clamped-Clamped-Free-Free (CCFF) boundary condition. The model used for this study is shown in Figs. 5 and 6.

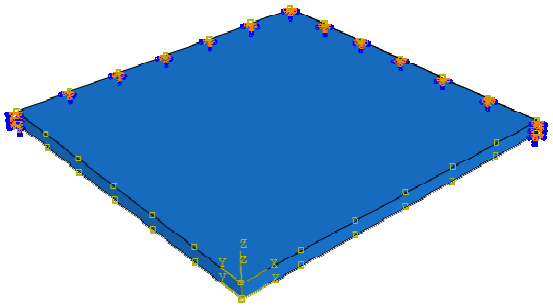

Fig. 5 Configuration of the smart adaptive sandwich plate with CCFF boundary condition

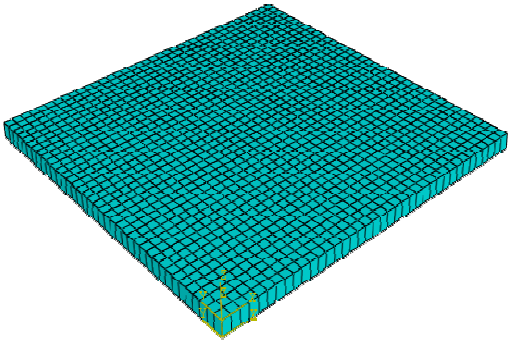

Fig. 6 Typical finite element model of the sandwich plate

A typical finite element model of the sandwich plate is shown in Fig. 6. It should be noted that the central piezoelectric layer consists of two layers of eight-node 3D linear brick piezoelectric elements (C3D8E), and each of the cover sheets consists of four-node doubly curved structural shell elements with reduced integration (S4R). The finite element mesh consists of 1444 elements for piezoelectric actuator and each cover aluminum sheets.

Fig. 7 shows the transverse displacement of the fixed-fixed-free-free square sandwich plate obtained by finite element analysis.

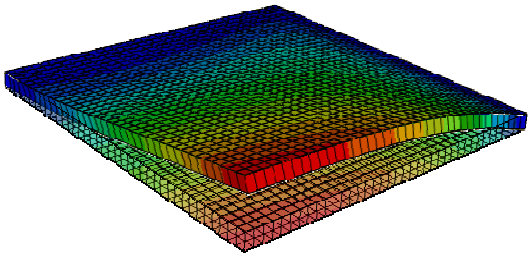

Fig. 7 Transverse displacement of the fixed-fixed-free-free sandwich plate by finite element analysis

It is shown that the transverse displacement obtained by the finite element analysis matches very well with the transverse displacement calculated by the Raleigh-Ritz method (presented by Zhang and Sun [6]). The transverse displacement obtained by the finite element analysis at the location $(L, L, 0)$ is 4.826×10^{-3} cm, which is only 0.041% different from the Raleigh-Ritz method ($p = 8$ and $q = 8$ case).

As it mentioned before, the orientation of poling vector has a significant effect on deflection and stress induced in the piezo-actuated adaptive sandwich plate. Therefore, we want to investigate the effect of poling vector angle on sandwich plate's deflection and stress induced. The poling vector angle is varied from $0-90^{\circ}$ with increment 5° ($\Delta\varphi = 5^{\circ}$). Fig. 8 shows the free tip displacement of CCFF plate vs. poling vector angle in horizontal direction.

International Science Index, Mechanical and Mechatronics Engineering Vol:8, No:5, 2014 waset.org/Publication/9998135

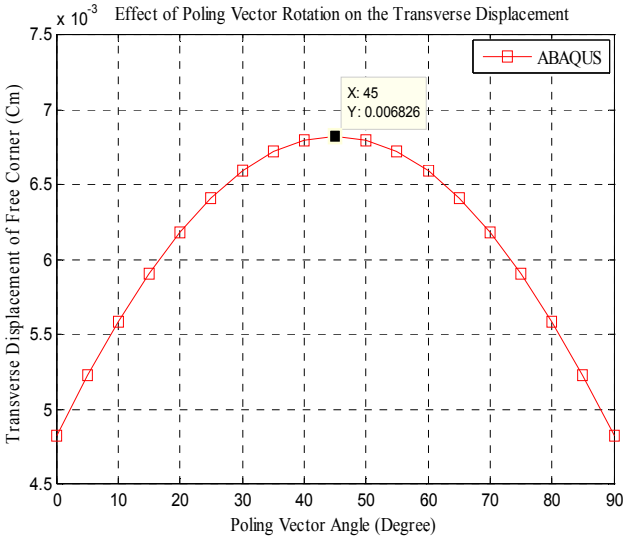

Fig. 8 Free tip displacement of CCFF plate vs. poling vector angle in horizontal direction

It is clear that the square sandwich plate is symmetric with respect to the diagonal of the plate along the poling direction. In other words, the square sandwich plate has a symmetric plane $y = x$. Therefore, the maximum transverse displacement of free corner has occurred at $\varphi = 45^{\circ}$.

Fig. 9 shows the maximum Von-Mises stress in CCFF sandwich plate vs. poling vector angle in horizontal direction.

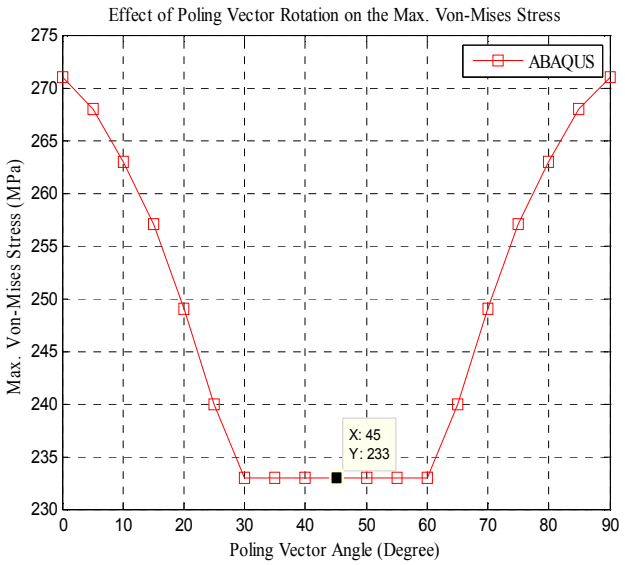

Fig. 9 Maximum Von-Mises stress in CCFF sandwich plate vs. poling vector angle in horizontal direction.

We can see from above figure that maximum Von-Mises stress is minimum at $\varphi = 45^{\circ}$. Also, the results confirm that maximum Von-Mises stress is not sensitive to poling vector angle from 30° to 60° for CCFF square sandwich plate. In this distance, the maximum stress is about $233\ MPa$.

Now, we want to investigate the effect of poling vector direction on deflection and stress induced in the piezo-actuated adaptive sandwich plate for a Simple-Simple-Free-Free (SSFF) boundary condition. The boundary configuration of the sandwich plate is shown in Fig. 10. The mesh used for this case is same as CCFF case. The finite element mesh consists of 1444 elements for piezoelectric actuator and each cover aluminum sheets.

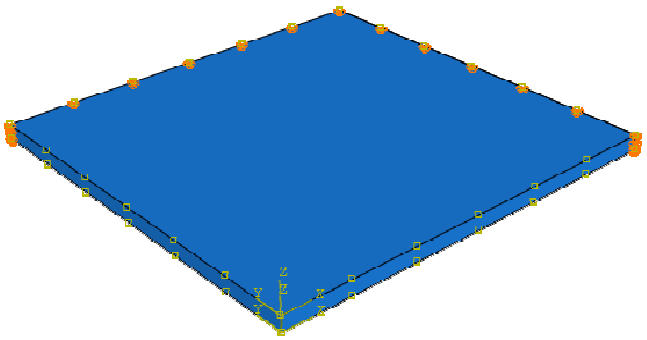

Fig. 10 Configuration of the smart adaptive sandwich plate with SSFF boundary condition

The transverse displacement obtained by the finite element analysis at the location $(L, L, 0)$ is 6.391×10^{-3} cm for SSFF boundary condition, which is greater than CCFF case. Fig. 11 shows the free tip displacement of SSFF plate vs. poling vector angle in horizontal direction.

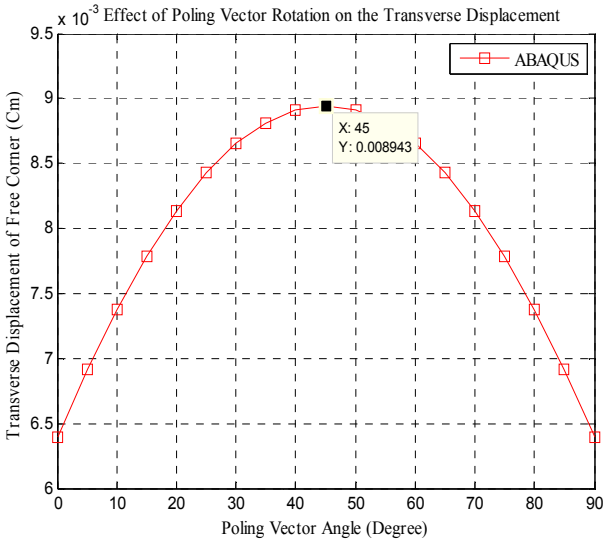

Fig. 11 Free tip displacement of SSFF plate vs. poling vector angle in horizontal direction

It is clear that the maximum transverse displacement of free corner has occurred at $\varphi = 45^{\circ}$ (the square sandwich plate has a symmetric plane $y = x$).

Fig. 12 shows the maximum Von-Mises stress in SSFF sandwich plate vs. poling vector angle in horizontal direction.

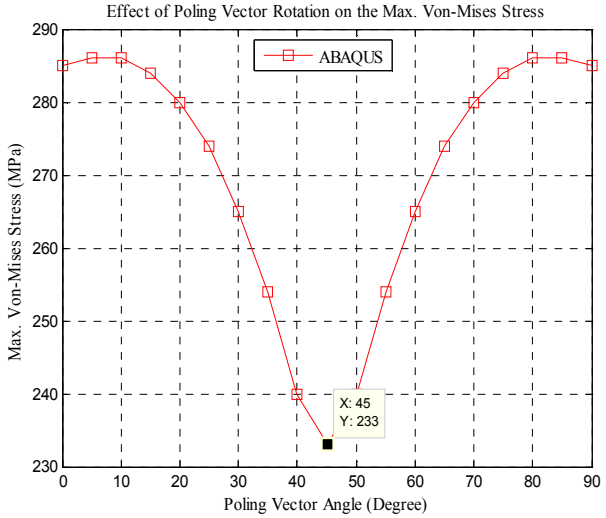

Fig. 12 Maximum Von-Mises stress in SSFF sandwich plate vs. poling vector angle in horizontal direction.

We can see from above figure that maximum Von-Mises stress is minimum at $\varphi = 45^{\circ}$. Also, the results confirm that maximum Von-Mises stress is not sensitive to poling vector angle from 5° to 10° and 80° to 85° for SSFF square sandwich plate. In this distance, the maximum stress is about $286\ MPa$. It is noticeable that CCFF and SSFF boundary conditions have the same maximum Von-mises stress at $\varphi = 45^{\circ}$.

X. Investigation of Other Polarized Ceramics

After deliberation of obtained results for PZT4 as a piezoceramic material, we want to study other polarized ceramics (piezoceramics) and their influences on the transverse displacement and stress induced in the piezo-actuated adaptive sandwich plate for both boundary conditions, CCFF and SSFF. Material constants of a few other polarized ceramics are given in the following tables [30]:

TABLE II
Mechanical Properties of a Few Polarized Ceramics

Material	c_{11}	c_{12}	c_{13}	c_{33}	c_{44}	c_{66}
PZT 5A	12.1	7.59	7.54	11.1	2.11	2.26
PZT 6B	16.8	8.47	8.42	16.3	3.55	4.17
PZT 5H	12.6	7.91	8.39	11.7	2.30	2.35
PZT 7A	14.8	7.61	8.13	13.1	2.53	3.60
PZT 8	13.7	6.99	7.11	12.3	3.13	3.36
$BaTiO_3$	15.0	6.53	6.62	14.6	4.39	4.24
			$\times 10^{10}\ N/m^2$			

TABLE III
Electrical Properties of a Few Polarized Ceramics

Material	e_{31}	e_{33}	e_{15}	ε_{11}	ε_{33}
PZT 5A	-5.4	15.8	12.3	0.811	0.735
PZT 6B	-0.9	7.1	4.6	0.360	0.342
PZT 5H	-6.5	23.3	17.0	1.505	1.302
PZT 7A	-2.1	9.5	9.2	0.407	0.208
PZT 8	-4.0	13.2	10.4	0.797	0.514
$BaTiO_3$	-4.3	17.5	11.4	0.987	1.116
		C/m^2		$\times 10^{-8}\ C/Vm$	

Table IV lists the transverse displacement at the location $(L, L, 0)$ for poling vector angle $\varphi = 45^{\circ}$. This angle is selected according to the previous results for both boundary conditions CCFF and SSFF. The bar charts of the obtained results are illustrated in Figs. 13 and 14.

TABLE IV
Free Tip Displacement of Sandwich Plate for Different Piezoceramics (CM)

Material	CCFF	SSFF
PZT 4	6.826×10^{-3}	8.943×10^{-3}
PZT 5A	7.620×10^{-3}	10.14×10^{-3}
PZT 6B	1.681×10^{-3}	2.174×10^{-3}
PZT 5H	9.682×10^{-3}	12.89×10^{-3}
PZT 7A	4.693×10^{-3}	6.071×10^{-3}
PZT 8	4.337×10^{-3}	5.681×10^{-3}
$BaTiO_3$	3.408×10^{-3}	4.429×10^{-3}

It is clear that PZT 5H has the most effect and PZT 6B has the least effect on the transverse displacement for both boundary conditions.

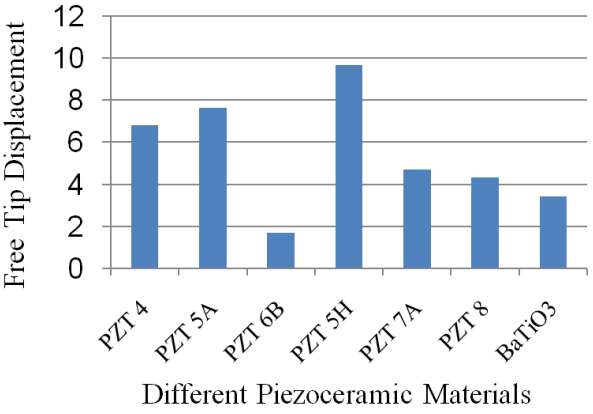

Fig. 13 Transverse displacement of free corner of CCFF plate for different piezoceramics

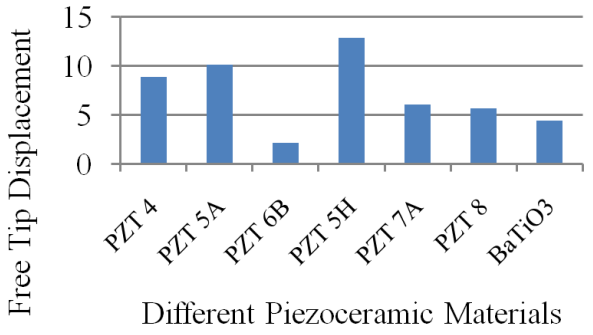

Fig. 14 Transverse displacement of free corner of SSFF plate for different piezoceramics

Table V lists the maximum Von-Mises stress for poling vector angle $\varphi = 45^{\circ}$.

International Science Index, Mechanical and Mechatronics Engineering Vol:8, No:5, 2014 waset.org/Publication/9998135

International Science Index, Mechanical and Mechatronics Engineering Vol:8, No:5, 2014 waset.org/Publication/9998135

TABLE V
MAXIMUM VON-MISES STRESS OF SANDWICH PLATE FOR DIFFERENT PIEZOCERAMICS (MPA)

Material	CCFF	SSFF
PZT 4	233	233
PZT 5A	213	213
PZT 6B	79.67	79.67
PZT 5H	294	294
PZT 7A	159	175
PZT 8	180	180
$BaTiO_3$	198	198

The bar charts of the obtained results are illustrated in Figs. 15 and 16.

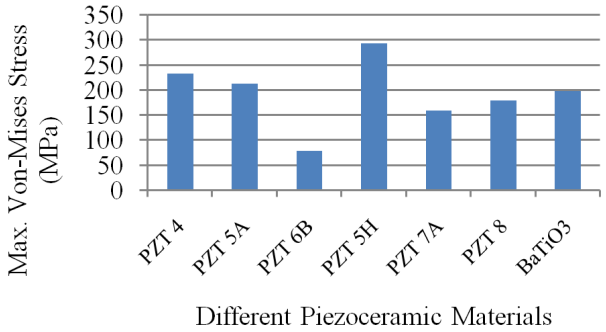

Fig. 15 Maximum Von-Mises stress of CCFF sandwich plate for different piezoceramics

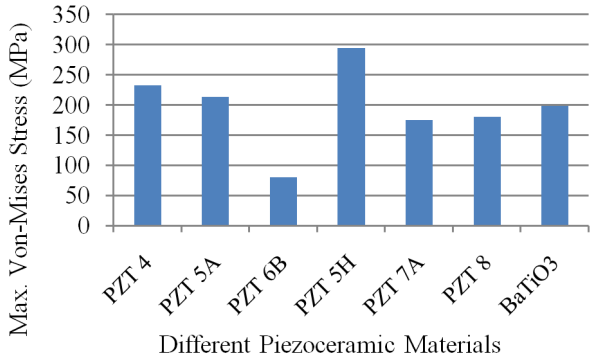

Fig. 16 Maximum Von-Mises stress of SSFF sandwich plate for different piezoceramics

It is clear that PZT 5H has the most effect and PZT 6B has the least effect on the maximum Von-Mises stress for both boundary conditions. Also, it could be seen that all piezoceramic materials have the same maximum stress for both boundary conditions CCFF and SSFF at poling vector angle $\varphi = 45^{\circ}$, with the exception of PZT 7A, which has the different values for CCFF and SSFF boundary conditions.

XI. CONCLUSIONS

An adaptive sandwich plate with a piezoelectric core is constructed using the shear mode of piezoelectric materials. Computationally efficient finite element models for a clamped-clamped-free-free and simple-simple-free-free sandwich plate based on the interfacial displacement continuity are developed. Clamped-clamped-free-free and simple-simple-free-free square sandwich plates are simulated by ABAQUS software (HKS 2005). It should be noted that in ABAQUS, the central piezoelectric layer consists of eight-node 3D linear brick piezoelectric elements (C3D8E), and each of the cover sheets consists of four-node doubly curved structural shell elements with reduced integration (S4R).

It is concluded that deflection and stress are much more in simple-simple-free-free sandwich plate than clamped-clamped-free-free boundary conditions. It is due to the looser constraint of SSFF square sandwich plate. Also, transverse displacement obtained in this study is compared with previous work for validation. The present model yields good results comparing with available results presented in the literature.

A numerical study of poling vector angle on plate performance was done. Transformed elastic, piezoelectric and dielectric matrices of transversely isotropic piezoceramic material derived by tensor transformation laws. It was shown that maximum plate deflection and minimum stress occurred when poling vector makes 45° with x axis (symmetric plane). It was also shown that maximum Von-Mises stress which occurs at closed edges of plate (simply supported or clamped), is not sensitive to poling vector angle from about $\theta = 5^{\circ}$ to 10° and 80° to 85° for SSFF square sandwich plate and from about $\theta = 30^{\circ}$ to 60° for CCFF sandwich plate.

Finally, several other piezoceramic materials were investigated for poling vector angle $\theta = 45^{\circ}$. It was shown that PZT 5H has the most effect and PZT 6B has the least effect on the transverse displacement and maximum Von-Mises stress for both boundary conditions. Therefore, PZT 5H is recommended as a shear-actuated mechanism for an adaptive sandwich plate, instead of PZT 4. Also, it was shown that all piezoceramic materials have the same maximum stress for both boundary conditions CCFF and SSFF at poling vector angle $\varphi = 45^{\circ}$, with the exception of PZT 7A, which has the different values for CCFF and SSFF boundary conditions.

REFERENCES

[1] Mitchell, J. A., and Reddy, J. N., (1995) "A refined hybrid plate theory for composite laminates with piezoelectric laminae", Int. J. Solids & Structures, Vol. 32, No. 16, pp. 2345-2367.
[2] Sun, C. T., and Zhang, X. D., (1995) "Use of thickness-shear mode in adaptive sandwich structures", Smart material and structures, Vol. 4, pp. 202-206.
[3] Zhang, X. D., and Sun, C. T., (1996) "Formulation of an adaptive sandwich beam", Smart material and structures, Vol. 5, pp. 814-823.
[4] Benjeddou, A., Trindade, M. A., and Ohayon, R., (1997) "A Unified Beam Finite Element Model for Extension and Shear Piezoelectric Actuation Mechanisms", Journal of Intelligent Material Systems and Structures, Vol. 8, No. 12, pp. 1012-1025.
[5] Reddy, J. N., (1999) "On laminated composite plates with integrated sensors and actuators", Engineering Structures, Vol. 21, pp. 568-593.
[6] Zhang, X. D., and Sun, C. T., (1999) "Analysis of a sandwich plate containing a piezoelectric core", Smart material and structures, Vol. 8, pp. 31-40.
[7] Benjeddou, A., (2000) "Advances in piezoelectric finite element modeling of adaptive structural elements: a survey", Computers and Structures, Vol. 76, pp. 347-363.
[8] Chee, C., Tong, L., and Steven, G.P., (2000) "A mixed model for adaptive composite plates with piezoelectric for anisotropic actuation", Computers and Structures, Vol. 77, pp. 253-268.
[9] Zhou, X., Chattopadhyay, A., and Thornburgh, R., (2000) "Analysis of Piezoelectric Smart Composites Using a Coupled Piezoelectric-

Mechanical Model", Journal of Intelligent Material Systems and Structures, Vol. 11, pp. 169-179.
[10] Bisegna, P., and Caruso, G., (2000) "Mindlin-Type Finite Elements for Piezoelectric Sandwich Plates", Journal of Intelligent Material Systems and Structures, Vol. 11, pp. 14-25.
[11] Huang, D., and Sun, B., (2001) "Approximate Analytical Solutions of Smart Composite Mindlin Beams", Journal of Sound and Vibration, Vol. 244, No. 3, pp. 379-394.
[12] Kapuria, S., (2001) "An efficient coupled theory for multilayered beams with embedded piezoelectric sensory and active layers", International Journal of Solids and Structures, Vol. 38, pp. 9179-9199.
[13] Vel, S. S., and Batra R. C., (2001) "Exact Solution for Rectangular Sandwich Plates with Embedded Piezoelectric Shear Actuators", AIAA Journal, Vol. 39, No. 7.
[14] Wang, Q., and Quek, S. T., (2002) "A Model for the Analysis of Beams with Embedded Piezoelectric Layers", Journal of Intelligent Material Systems and Structures, Vol. 13, pp. 61-70.
[15] Aldraihem, O. J., and Khdeir, A. A., (2003) "Exact deflection solutions of beams with shear piezoelectric actuators", International Journal of Solids and Structures, Vol. 40, pp. 1-12.
[16] Lesieutre, G. A., Loverich, J., Koopmann, G. H., and Mockensturm, E. M., (2004) "Increasing the Mechanical Work Output of an Active Material Using a Nonlinear Motion Transmission Mechanism", Journal of Intelligent Material Systems and Structures, Vol. 15, pp. 49-58.
[17] Garcia Lage, R., Mota Soares, C. M., Mota Soares, C. A., Reddy, J. N., (2004) "Modeling of piezolaminated plates using layerwise mixed finite elements", Computers and Structures, Vol. 82, pp. 1849-1863.
[18] Kapuria, S., and Achary, G.G.S., (2005) "A coupled consistent third-order theory for hybrid piezoelectric plates", Composite Structures, Vol. 70, pp. 120-133.
[19] Azulay, L., E., and Abramovich, H., (2005) "Rectangular Composite Plates with Extension and Shear Piezoceramic Layers and Patches", TAE Report, No. 951, Faculty of Aerospace Engineering, Israel Institute of Technology.
[20] Polit, O., and Bruant, I., (2006) "Electric potential approximations for an eight node plate finite element", Computers and Structures, Vol. 84, pp. 1480-1493.
[21] Robaldo, A., Carrera, E., Benjeddou, A., (2006) "A unified formulation for finite element analysis of piezoelectric adaptive plates", Computers and Structures, Vol. 84, pp. 1494-1505.
[22] Balamurugan, V., and Narayanan, S., (2007) "A piezoelectric higher-order plate element for the analysis of multi-layer smart composite laminates", Smart Material and Structure, Vol. 16, pp. 2026-2039.
[23] Sheng, H. Y., Wang, H., and Yea, J. Q., (2007) "State space solution for thick laminated piezoelectric plates with clamped and electric open-circuited boundary conditions", International Journal of Mechanical Sciences, Vol. 49, pp. 806-818.
[24] Ren, L., (2007) "Theoretical study on shape control of thin cross-ply laminates using piezoelectric actuators", Composite Structures, Vol. 80, pp. 451-460.
[25] HKS, (2005) "ABAQUS User's Manual version 6.7", (Providence, RI: Hibbitt, Karlsson, and Sorenson).
[26] Meitzler, A. H., Tiersten, H. F., Warner, A. W., Berlincourt, D., Couqin, G. A., and Welsh, F. S., (1987) III, "IEEE Standard on Piezoelectricity", ANSI/IEEE Std 176-1987, New York.
[27] Tiersten H F (1969) "Linear Piezoelectric Plate Vibrations", (New York: Plenum) pp. 33-9.
[28] Sadd, M. H., (2005) "Elasticity; Theory, Application and Numerics", Elsevier Butterworth-Heinemann.
[29] Mase, G. T., and Mase, G. E., (1999) "Continuum mechanics for engineers", 2nd ed., CRC press, pp. 42-44.
[30] Yang, J. S., (2005) "An Introduction to the Theory of Piezoelectricity", Springer.

International Science Index, Mechanical and Mechatronics Engineering Vol:8, No:5, 2014 waset.org/Publication/9998135